Aeolian Research 10 (2013) 61–76

Contents lists available at SciVerse ScienceDirect

Aeolian Research

journal homepage: www.elsevier.com/locate/aeolia

# The influence of mineral detritus on rock varnish formation

Ronald I. Dorn [a,*], David H. Krinsley [b], Kurt A. Langworthy [c], Jeffrey Ditto [c], Tyler J. Thompson [a]

[a] School of Geographical Sciences and Urban Planning, Arizona State University, Tempe, AZ 85287-5302, USA
[b] Department of Geological Sciences, University of Oregon, Eugene, OR 97403-12723, USA
[c] CAMCOR, Department of Chemistry, University of Oregon, Eugene, OR 97403-1241, USA

ARTICLE INFO

*Article history:*
Received 2 March 2013
Revised 25 April 2013
Accepted 25 April 2013
Available online 21 May 2013

*Keywords:*
Dust
Diagenesis
Manganese
Rock coating
Weathering

ABSTRACT

A mix of high resolution electron microscope methods imaged the textures and chemistry of rock varnish samples from 19 field sites on five continents. The vast majority of aeolian mineral is not incorporated into manganiferous rock varnish. Of those dust particles that are enveloped, submicron sized oval-shaped quartz minerals are the most common type of detritus seen, as they rest conformably between laminated layers. The dominance of quartz as the most common detrital mineral, combined with the relative rarity of feldspars – is consistent with the hypothesis that feldspars experience *in situ* decay into clay minerals. After the detritus is buried in varnish, mineral boundaries often develop enhanced porosity. Some porous zones around dust particles develop submicron skins of redeposited Mn–Fe. In other cases, the porous zones aid in the transport of capillary water that mobilizes and redeposits Mn–Fe as stringers in fissures. Larger dust particles ~10 μm in diameter are deposited in microtopographic depressions, such as tubes created by acid-producing lithobionts. Varnishes growing in particularly dusty regions form alternating dust-rich and varnish-rich layers that potentially correlate to alternating dusty and less dusty periods. The very foundation of varnish, the underlying rock, is often less stable in the surficial environment than varnish – leading to enhanced porosity and mineral decay in the substrate. Sometimes, physical collapse of varnish into the underlying void space mixes varnish and rock; more commonly, however, remobilization of varnish constituents into these pore spaces creates case hardening of the weathering rind in the underlying rock.



## 1. Introduction

The influence of the underlying rock on the formation of rock (or desert) varnish has been a controversial topic. von Humboldt (1812) postulated that submillimeter manganese-rich coatings formed as a deposit on top of the rock (Dorn et al., 2012c; von Humboldt, 1812). Researchers advocating von Humboldt's accretionary hypothesis, however, were rare (Basedow, 1914; Francis, 1921; Klute and Krasser, 1940; Krumbein, 1969) prior to the use of electron microscopy. There existed a clear consensus throughout much of the late 19th and 20th centuries that the constituents of "desert varnish" – as most called it – derived from solutes mobilized from decayed mineral matter in the underlying rock (Bard et al., 1978; Birot, 1969; Blake, 1905; Engel and Sharp, 1958; Glennie, 1970; Holmes, 1965; Hume, 1925; Hunt, 1954; Linck, 1901, 1928; Longwell et al., 1950; Lucas, 1905; Marshall, 1962; Merrill, 1898; Peel, 1960; Walther, 1891; Wilhelmy, 1964; Woolnough, 1930).

As can be the case in science, the clear consensus turned out to be wrong, but it required a new technique to change perspective. Just as the use of satellite imagery played a role in recognizing the role of catastrophic flooding (Bretz, 1923) on the channeled scablands (Baker and Bunker, 1985), the use of different electron microscope techniques supported von Humboldt's accretionary hypothesis (e.g. Fig. 1) through the visualization of very clear contacts between the depositing varnish and underlying minerals (Potter and Rossman, 1977). Continued research using light (Liu and Broecker, 2000, 2008a; Perry and Adams, 1978), secondary (Dorn, 1986; Dorn and Oberlander, 1982), back-scattered (BSE) (Dorn, 2009a; Krinsley et al., 1990), and high resolution transmission electron microscopy (HRTEM) (Krinsley, 1998; Krinsley et al., 1995, 2009) led to a new consensus that manganese-rich subaerial rock varnish is an aeolian deposit.

Since this latest shift in consensus back to von Humboldt's (1812) accretionary hypothesis, relatively little concern has been paid to the role of rock material – whether the underlying rock or aeolian mineral particles – on varnish formation. Research on the influence of the rock has been limited to rock-spalling events that also remove rock coatings (Etienne, 2002; Gordon and Dorn, 2005; Tratebas et al., 2004; Turkington and Paradise, 2005) and case hardening (Conca, 1982; Conca and Rossman, 1982; Dorn

* Corresponding author.
*E-mail addresses:* ronald.dorn@asu.edu (R.I. Dorn), krinsley@uoregon.edu (D.H. Krinsley), klangwor@uoregon.edu (K.A. Langworthy), ditto@uoregon.edu (J. Ditto), tjthomp9@asu.edu (T.J. Thompson).

1875-9637/$ - see front matter © 2013 Elsevier B.V. All rights reserved.
http://dx.doi.org/10.1016/j.aeolia.2013.04.005

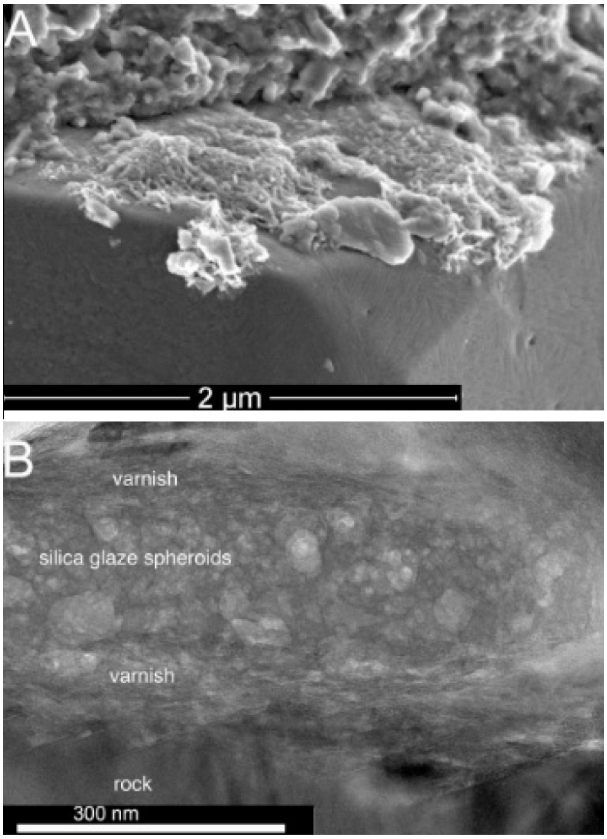


**Fig. 1.** Clear contact between varnish deposited on relatively fresh minerals of the underlying rock. (A) Secondary electron image of manganese-rich rock varnish formed on quartz collected from von Humboldt's research site along the cataracts of the Orinoco River between the missions of Carichana and Santa Barbara (von Humboldt, 1812, pp. 242–246); source: Dorn et al. (2012c). (B) HRTEM image of varnish deposited on the underlying rock (darker material at the bottom of the image). Layered rock varnish forms a 50 nm thick deposit, followed by accretion of silica glaze spheroids, and then a return to layered rock varnish; source: Langworthy et al. (2010).

et al., 2012a; Washburn, 1969). In this paper, however, we postulate that aeolian detrital minerals deposited on rock surfaces are subsequently enveloped, altering varnish formation and its diagenesis. In evaluating this hypothesis, we use samples from different environmental settings and we employ a variety of electron microscope techniques.

The next section of this article provides a background of current thinking on rock (or desert) varnish formation. The methods section describes sampling sites, sample preparation methods, and the different electron microscopic techniques employed. An integrated results and discussion section presents imagery in microstratigraphic order from the top (youngest) to the bottom (oldest) of varnish, analyzing interactions between aeolian mineral detritus from the 'dust cycle' (Shao et al., 2011) with rock varnish processes.

## 2. Overview of rock varnish formation

The literature on rock (or desert) varnish formation contains four general types of conceptual models graphically portrayed in Fig. 2. One model (Fig. 2A) involves abiotic enhancement of manganese relative to iron, explaining the Mn:Fe ratio in varnish that is 60 times greater than that found in the underlying rock or dust, which results from cycles of acid solutions separating Mn (II) followed by oxidizing conditions concentrating Mn in varnish (Engel and Sharp, 1958; Hooke et al., 1969; Smith and Whalley, 1988).

Another set of hypotheses purport that lithobionts or their organic remains (e.g. spores, polysaccharides, oxides, humic substances) play a role in binding varnish and concentrating manganese and iron (e.g. Fig. 2B) (Allen et al., 2004; Gorbushina, 2003; Krumbein, 1969; Kuhlman et al., 2006; Parchert et al., 2012; Perry et al., 2003; Scheffer et al., 1963; Staley et al., 1983; White, 1924). A third hypothesis argues that silica binding of detrital grains, organics, and aerosols (Dorn, 2007a; Perry and Kolb, 2003; Perry et al., 2006; Perry and Sephton, 2007) results in varnish formation (Fig. 2C).

We favor a polygenetic model (Fig. 2D) focusing on clay–bacteria-interactions (Dorn, 1998; Dorn and Krinsley, 2011; Dorn et al., 1992; Krinsley, 1998); varnish formation starts with the oxidation and concentration of Mn (and Fe) by bacteria. Wetting events dissolve nanometer-scale fragments of Mn. Ubiquitous desert dust supplies interstratified clay minerals. The Mn-bacterial fragments fit into the weathered edges of clays, playing a role much like mortar cementing a brick wall. All four mechanisms are reviewed and compared in detail elsewhere (Dorn, 2007b, 2009a).

The polygenetic model (Fig. 2D) starts with physical attachment of dust particles held onto rock surfaces (Bishop et al., 2002; Ganor et al., 2009; Jordan, 1954). Then, bacteria concentrate manganese and iron (Dorn, 2007b; Dorn and Oberlander, 1981; Grote and Krumbein, 1992; Hungate et al., 1987; Krinsley et al., 2012; Northup et al., 2010; Palmer et al., 1985; Wang et al., 2011). While some bacterial sheaths survive as in tact microfossils (Dorn, 1998; Dorn and Meek, 1995; Krinsley, 1998), most break down into fragments that then dissolve (Krinsley, 1998). This ongoing diagenesis of Mn–Fe casts release nanometer-scale fragments seen in HRTEM as having a granular texture. Fixation of the Mn occurs only a few nanometers away as hydroxides are mobilized into mixed-layered clays (Potter, 1979).

The rate of varnish formation can vary tremendously, depending on the macroenvironment and microenvironment of sampling. For the types of locations best suited for analyzing microlaminations, rates of formation are typically microns per millennia (Dorn, 1998; Liu and Broecker, 2000). However, more mesic locales can produce rates of formation on the order of microns per century (Dorn et al., 2012b; Krinsley et al., 2012; Spilde et al., 2013) – high enough to preserve Mn-enhancing bacteria microfossils (Dorn and Meek, 1995). Because the vast majority of varnish takes millennia to accrete microns, Mn-enhancement must be extraordinarily rare, contributing a few cell-wall crusts of manganese per millennia (Dorn and Krinsley, 2011). Even the higher rates of formation would preclude a role for the vast majority of organisms found in association with varnish (Allen et al., 2004; Krumbein, 1969; Kuhlman et al., 2006; Parchert et al., 2012; Perry et al., 2003; Scheffer et al., 1963; Staley et al., 1983; White, 1924), because typical formation rates would be microns per year if all of this organic activity truly played a role in varnishing (Dorn and Krinsley, 2011).

The importance of ongoing diagenesis, after the initial aggradation of clays and bacteria, has been recognized as a key process, well after the initial redistributing Mn from bacterial sheaths to clay minerals. Many electron microscopy-viewed textures are produced by ongoing dissolution and reprecipitation of oxides. Organic acids (Dragovich, 1987, 1993) dissolves oxides and leach cations from pockets with porous textures (Dorn and Krinsley, 1991; Krinsley et al., 1990), where the dissolved Mn and Fe precipitates along the rims these pores (Garvie et al., 2008; Krinsley et al., 1990). The redistribution of Mn and Fe in capillary channels forms crosscutting submicron Mn stringers and wider cracks filled with oxides (Garvie et al., 2008; Krinsley et al., 1990).

Despite considerable prior work on varnish formation and its subsequent diagenesis, this article's focus turns towards a topic not explored previously in the varnish literature: the influence of mineral dust on varnish formation and subsequent diagenesis. Cer-

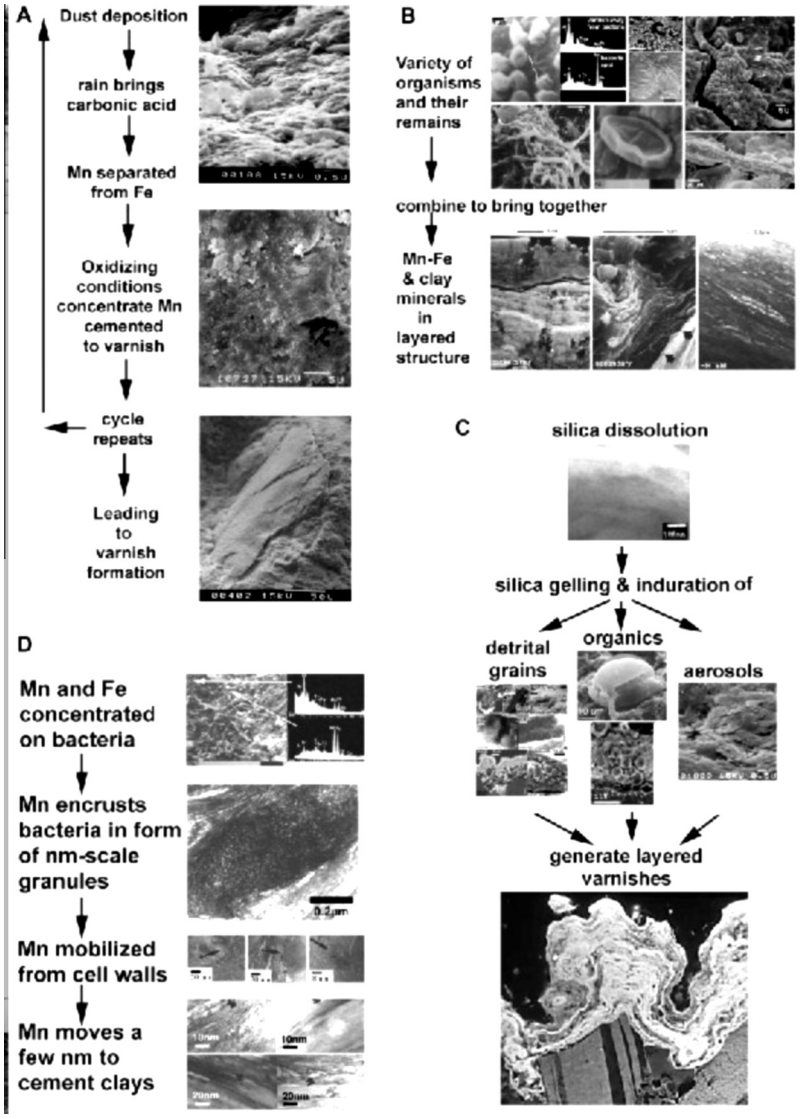


**Fig. 2.** Four conceptual models of rock varnish formation (Dorn, 2007b): (A) abiotic enhancement; (B) lithobionts or their organic remains binding varnish and concentrate Mn and Fe oxides and oxyhydroxides; (C) silica binding of detrital grains, organics, and aerosols; and (D) polygenetic clay–bacteria-interactions.

tainly, many researchers have made the general observation that fragments of rock material occur in the accumulating varnish (Haberland, 1975; Krinsley et al., 1990; Krumbein, 1969; Lucas, 1905; Soleilhavoup, 1986), and some have explored links between these fragments and particular sources such as volcanic events (Harrington, 1988). Discussions about the inclusion of mineral detritus in rock coatings is not exclusive to rock varnish, as mineral detritus occurs in sulfate crusts (Sanjurjo-Sánchez, 2010), carbonate crusts (Khalaf and AlShubaibi, 2012), silica glaze (Mantha et al., 2012), phosphate skins (Brook et al., 2011), and other rock coatings (Dorn, 1998). However, no prior research has yet focused on the importance of aeolian mineral dust in rock varnish formation and diagenesis.

## 3. Methods

### 3.1. Sampling sites

This study involves the analysis of samples from a variety of collection sites, including warm desert sites such as Death Valley and the Sonoran Desert to cold desert locales such as Antarctica and the Tibetan Plateau (Table 1). The imagery examined here was mined from a variety of research projects conducted over the past three decades. While site selection was driven by other research questions, the variety of collection locales makes it possible to compare varnishes from very different environmental settings.

### 3.2. Electron microscope techniques

We employed several electron microscopy techniques to image and analyze our specimens (Table 2). Samples were prepared in a variety of ways, allowing us to perform light microscopy prior to electron microscopy to aid in locating regions of interest. Sample preparation included: thin sections, polished epoxy-embedded rock chips, and raw rock chips placed directly into the SEM. To alleviate specimens from charging under the electron beam, some were coated with ~20 nm of thermally evaporated carbon while others were locally grounded by using an Omniprobe micromanipulator (Ditto et al., 2012).

Many samples were imaged and analyzed with high resolution TEM microscopy that required thinning samples enough to permit electrons to pass through them with an 80 and 300 kV electron

**Table 1**
Basic information on the sampling sites analyzed.

| Figures | Lat/long | Description of sampling site |
|---|---|---|
| 1A, 23A | N 6.24 W 67.40 | Splash zone of cataracts of Orinoco River, from the approximate field location studied by von Humboldt, collected by Francis Record |
| 1B, 6, 19B, 23A | N 35.70 E 81.58 | Ventifacted and then varnished trachyandesite lava flows of the Ashisan volcano, Ashikule Basin, Tibetan Plateau. In addition to rock varnish, silica glaze is a common rock coating. The adjacent playa generates abundant alkaline dust |
| 3 | N 43.98 E 74.23 | Glacial boulder exposed to the subaerial environment at Adirondack Park Preserve, New York. Sample collected by Barry DiGregorio |
| 4 | Location confidential | This petroglyph site has been closed to the public, to protect the priceless rock art in the Black Hills, Wyoming. The sandstone cliff faces host varnished petroglyphs, silica glaze and iron films |
| 5, 7, 20, 21, 23D | N 33.25 W 111.34 | Desert pavement next to the Pinal Pioneer Parkway, Sonoran Desert. The desert pavement rests on a stream terrace. Clast sizes range from boulders (sampled) to sand particles |
| 8, 9, 12 and 16, | N 36.24 W 116.89 | 2 m diameter boulder on Hanaupah Canyon alluvial fan, Death Valley. The boulder was carried by a debris flow and rests in a desert pavement largely consisting of smaller clasts |
| 10 | Location confidential | The Panaramitee petroglyph site in South Australia consists of a wide array of carvings into silicified dolomite. The semi-arid environment includes rock coatings of varnish, iron film, silica glaze, phosphate films, and lithobionts |
| 11, 19A, 23C | N 33.57 W 112.01 | Bedrock outcrop of schist, Phoenix Mountains Preserve, Sonoran Desert. The varnish likely started out inside a rock crevice that spalled open |
| 13 | N 35.20 W 115.87 | Basalt flow surface, Cima Volcanic Field, Mojave Desert. The a'a' texture was sampled from this late Pleistocene flow |
| 14 | N 43.20 W 78.55 | Boulders used in construction of the Erie Barge Canal, New York between 1908 and 1917. Water splash is unlikely |
| 15 | N. 36.74 W 116.51 | Colluvial boulder, ignimbrite, Yucca Mountain, Nevada. The meter-sized boulder exists in a field of similarly sized clasts |
| 16, 18A | S 14.59 W 75.12 | Desert pavement, Nazca, Peru. The clast was sampled from inside a trapezoidal geoglyph form |
| 16 | S 76.96 W 143.78 | Clark Mountains, Marie Byrd Land, Antarctica, from the Texas Tech University Antarctic collection |
| 16 | N 19.84 W 115.93 | Holocene lava flow, Hawai'i. Most of the lava flow is coated in silica glaze. Only small pockets of manganiferous varnish exists |
| 17 | S 23.72 E 113.85 | Bedrock outcrop, hogback, near Alice Springs, Australia. The sample was collected from a resistant quartzite ridge. |
| 18B | N 34.35 E 8.89 | Argillite clast from the Oued es Seffaia alluvial fan, on the south flank of Djebel Orbata, Southern Atlas, collected by N. Drake |
| 18C | N 30.35 E 34.95 | Desert pavement cobble, Negev Desert, Israel. The desert pavement mostly consists of small cobbles |
| 18D | N 29.29 E 34.73 | Alluvial-fan quartzite boulder embedded in a desert pavement, Sinai Peninsula, Egypt |
| 22 | N 31.95 W 111.63 | Granitic bedrock outcrop, near the summit of Kitt Peak, Arizona. The bedrock surface is largely covered in lithobionts. However, patches of rock varnish exist on the scale of centimeters |

**Table 2**
Microscopy techniques used in this research.

| Technique (and acronym) | Information obtained | Spatial resolution | Limitations |
|---|---|---|---|
| Coupled dual-beam focused ion beam electron microscopy (FIB-EM) | Used to create and image cross-sections *in situ*, widely used to extract sections for TEM analysis. Real time imaging in SEM mode during ion milling | >∼1 nm | Maximum sample and scan size, requires vacuum, Ga ion implantation |
| High resolution transmission electron microscopy (HRTEM) | 2-D spatial imaging, lattice imaging | >0.08 nm | Small area, sample preparation challenges, sample thickness < 50 nm |
| Energy dispersive X-ray analysis (EDX) | Elemental composition, X-ray mapping of elements | >1 nm (HRTEM); >20 nm (SEM) | Detection limit varies, ∼0.2 wt%. Difficult for light element detection |
| Scanning electron microscopy (SEM) with back-scattered electron detector (BSE) | Average atomic number (Z) revealed through contrast I grayscale image | >5 nm | Generally requires vacuum (dry samples), sample size dependent on chamber size |
| Scanning electron microscopy (SEM) with secondary electrons (SE) | 2-D spatial imaging | >1 nm | Requires vacuum, sample size dependent on chamber size |

beam. To prepare specimens for high-resolution TEM studies, a dual-beam focused ion beam microscope (FIB-SEM) was used to ion mill, and lift out a region of interest. The region of interest was then transferred *in situ* using an Omniprobe micromanipulator, to a copper TEM grid. The region of interest was then thinned using low ion beam currents until the specimen was ∼50 nm thick (Brown and Lee, 2007).

The Titan 80–300 kV HRTEM used in our study was equipped with a high angle annular dark-field STEM detector, allowing us to easily recognize regions of interest based on atomic number (Z) contrast (Wang and Cowley, 1989). Compositional analysis employed energy dispersive X-ray spectroscopy (EDX). The high voltage, along with the thin TEM sample reduced the excitation volumes in our specimen allowing EDX measurements to be made with spot sizes of <10 nm (Goldstein et al., 2003).

## 4. Results and discussion

Our findings are compiled here microstratigraphically from top to bottom. We start by examining of the envelopment of particles by varnish accretion, followed evaluating interactions between the mineral detritus and in the middle of varnish. Then, we examine interactions along the varnish – underlying rock boundary.

### 4.1. Initial envelopment of aeolian mineral detritus

The vast majority of mineral dust that falls onto surfaces (Fig. 3) is not enveloped by manganiferous rock varnish; otherwise rates of varnish accretion would be $10^2$ to $10^4$ times faster than typically observed (Dorn and Krinsley, 2011). A lot of material can end up forming a transient deposit on varnish surfaces (Fig. 4). In rare circumstances, the clay–Mn–Fe matrix of varnish envelopes detrital mineral grains (Figs. 5–7). Given that varnish can be as thin as a few tens of nanometers (Fig. 7) removal of loosely adhered particles could occur by rainsplash, overland flow, or even deflation.

We hypothesize that mineral detritus envelopment occurs more frequently in an environment of abundant dust, because the timing of varnish accretion must correspond with the presence of mineral dust. This is the case in central Arizona where historical land use change has promulgated dusty conditions (Fig. 5) and at locations near natural playas with abundant dust (Figs. 6 and 7).

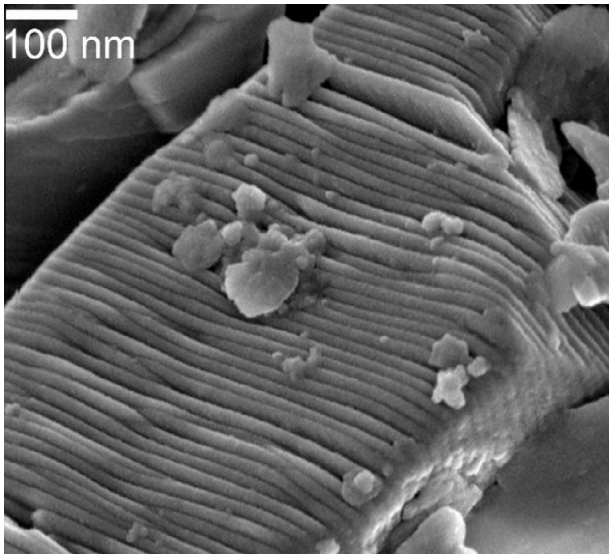


**Fig. 3.** Mineral decay creates nanotopographic irregularities seen in this SEM image of dust particles attracted to the underlying biotite (based on EDX data) surface, Adirondack Park, New York.

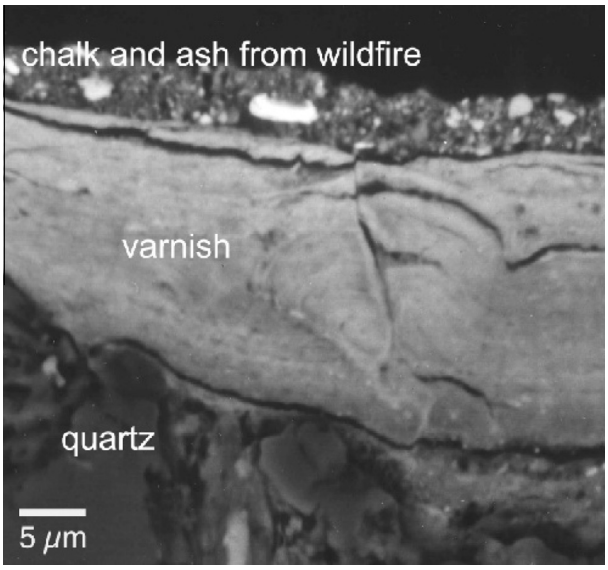


**Fig. 4.** BSE image of a chalked petroglyph at Whoop-up Canyon, Wyoming. The chalk is mixed with soot from a wildfire, and this mixture adheres to the rock varnish. However, there is no clear evidence of envelopment in this image. The soot and chalk just appears to rest on the varnish surface.

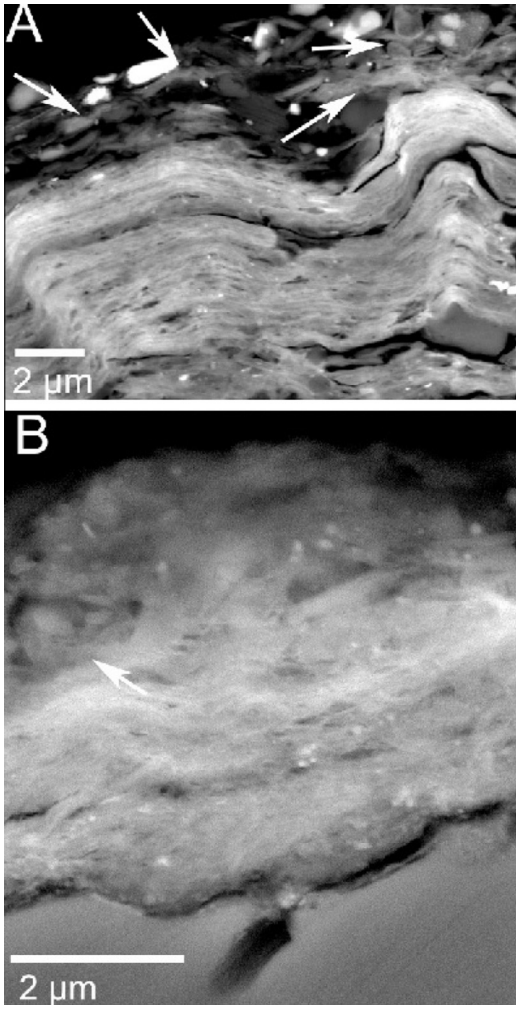


**Fig. 5.** The surface of varnish from near Florence, Arizona, exemplified in two different views, displays a surficial layer with mineral detritus partially envelopment by layered varnish. Some laminated varnish (arrows in A) has deposited in and amongst the minerals to loosely cement the detritus to the underlying laminated varnish. Some bits of quartz (arrow in B) seem to create a void space around the mineral, perhaps from capillary water flow. The less focused upper portion of image B likely reflects sample preparation issues. It is possible that the sudden change from laminated to detrital-rich layers reflects the historical land use change in the area of central Arizona that has increased dust abundance (Marcus and Brazel, 1992).

In Figs. 5 and 6 some of the mineral detritus appears to be loosely cemented by poorly organized varnish. We speculate that patches of laminated varnish interacts with capillary and hygroscopic water to redistribute Mn–Fe that loosely cements detrital aeolian grains. It is possible that the high porosity of the upper varnish layer gradually infills from remobilized Mn–Fe. However, such a hypothetical process would produce chaotic textures lower in the varnish stratigraphy – a texture that only rarely occurs. Thus, we speculate that in particularly dusty areas, this admixture of varnish and mineral detritus periodically spalls from the laminated varnish underneath. Then, the enveloped detrital minerals that were not a part of this spalled layer would end up being a part of the surviving varnish microstratigraphy.

What survives such a hypothetical spalling event could be determined by the nature of the connection between detrital grain

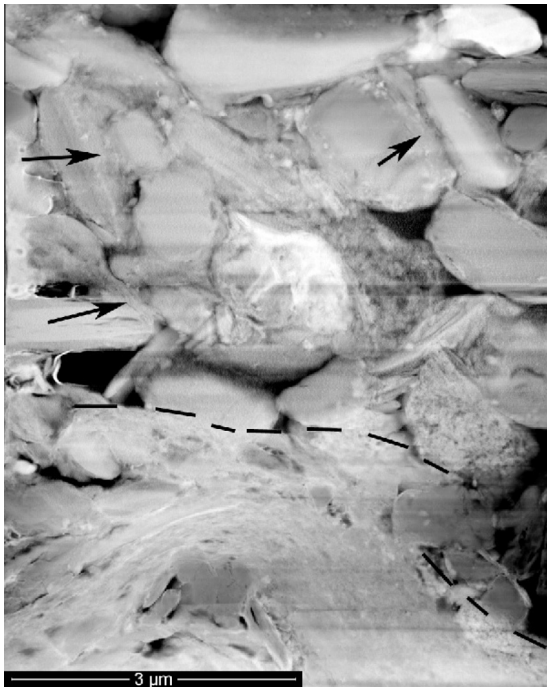


**Fig. 6.** A FIB section imaged with TEM of Ashikule Basin varnish, Tibet, where area beneath the black dashed line is dominated by the clay–Mn–Fe laminated matrix of rock varnish. Above this varnish-dominated zone is a quartz-rich layer with abundant detritus. We note nanoscale coatings on most of the detrital particles. In many places (e.g. arrows), a mixture of clay–Mn–Fe varnish penetrates into intergrain areas. This mixed texture of pockets of varnish and detrital minerals is consistent with the movement of capillary water through pore spaces, with subsequent movement of water involved in the precipitation of Mn–Fe remobilized from laminated varnish.

and varnish. The polygenetic model of varnish formation discussed previously (Fig. 2D) posits that Mn-encrusted bacterial casts break down into granular-textured fragments (Dorn, 2007b; Krinsley, 1998). Then, Potter (1979, pp. 174–175) proposed:

> "Deposition of the manganese and iron oxides within the clay matrix might then cement the clay layer . . . the hexagonal arrangement of the oxygens in either the tetrahedral or octahedral layers of the clay minerals could form a suitable template for crystallization of the layered structures of birnessite. The average 0–0 distance of the tetrahedral layer is 3.00 Å in illite–montmorillonite mixed-layered clays, which differs only 3.4% from the 2.90 Å distance of the hexagonally closed-packed oxygens in birnessite . . ."

The polygenetic model of rock varnish formation includes the concept that the manganese minerals in varnish remain unstable (McKeown and Post, 2001) and our observations at the nanoscale (Dorn, 1998; Dorn and Krinsley, 2011; Dorn et al., 2012c; Krinsley, 1998; Krinsley et al., 2009, 2012; Krinsley and Rusk, 2000) suggest that the source of the manganese appears to be bacteria cell walls that break down and release nanometer fragments for mobilization into the feathered edges of weathered clays (Robert and Tessier, 1992).

BSE images of quartz minerals that are enveloped into varnish sometimes show a white rim of oxides of manganese and iron, as revealed by EDX analyses (Fig. 8). When examined at higher resolutions, Fig. 9 shows that granular-textured varnish occurs between laminated varnish and quartz mineral detritus. In HRTEM imagery from Death Valley (Fig. 9), bacterial cast fragments appear to release nanometer-scale granules that are found in direct contact with the detrital quartz grains. As the oxide-encrusted cell wall breaks up, these granular clusters are slowly dissolved and are eventually remobilized into clay minerals (Dorn, 1998; Krinsley, 1998). Thus, we hypothesize that at least some of the detrital grains are enveloped because ongoing diagenesis of varnish constituents helps cement detrital grains.

The envelopment of detrital grains could involve a variety of organisms that dissolve the Mn–Fe cement of varnish such as lichens (Dragovich, 1986), microcolonial fungi (Dragovich, 1993; Fabero-Longo et al., 2011), and other rock-surface organisms (Gadd, 2007; Gorbushina, 2007; Hirsch et al., 1995; Viles, 1995). We commonly observe tube-like depressions associated with microcolonial fungi, suggesting that these depressions can have a biotic origin. These surface depressions collect mineral detritus (Fig. 10), that is then sealed by accreting laminated varnish (Fig. 11).

The microtopography of the detrital grain might also play a role in its envelopment into varnish. Mineral grains with an etched nanoscale microtopography (Fig. 12) could experience enough electrostatic or intermolecular force between the surfaces in contact (Bishop et al., 2002; Ganor et al., 2009; Jordan, 1954) to allow particles to rest in place long enough to be incorporated by accreting varnish.

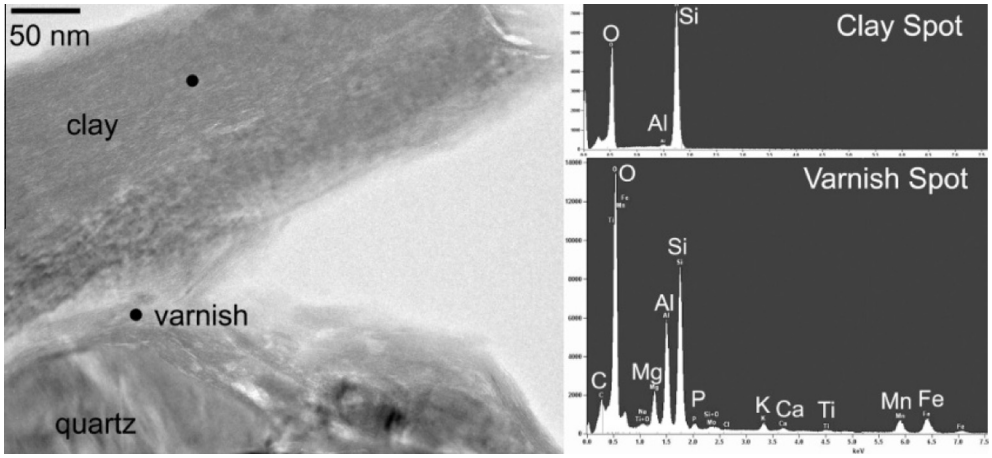


**Fig. 7.** Grain-cementing varnish seen at the micron-scale in Fig. 5 appears to be distributed irregularly on nanometer-grain surfaces. Rock varnish appears to bind clay minerals to detrital grains such as quartz. The low levels of C in the EDX analyses is typical of varnish overall (Dorn and DeNiro, 1985).

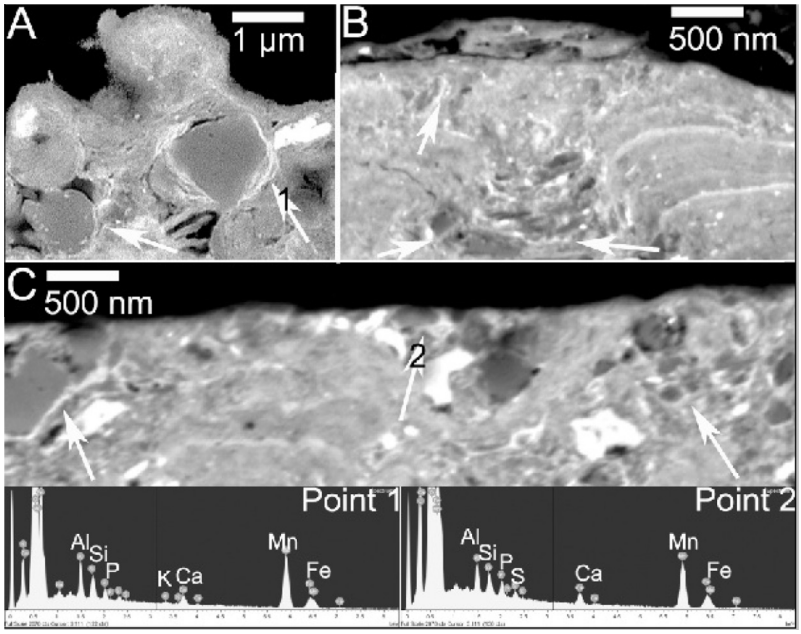


**Fig. 8.** BSE images of quartz mineral grains enveloped by varnish collected from Dath Valley, where arrows highlight white rims of oxides partially surrounding detrital grains. Example EDX spectra at point 1 in image A and point 2 in image C reveal high concentrations of Mn and Fe.

### 4.2. Submicron detrital minerals within layers

The previous section's emphasis on a particle's initial envelopment into varnish should not imply that the upper layers of varnish are dominated by detrital minerals. In fact, most of the varnishes we have analyzed do not contain a detrital-rich surface layer. Figs. 13–15 show a more typical circumstance where submicron fragments rest somewhat conformably between varnish layering. This subparallel orientation could potentially relate to water movement on subaerial varnish surfaces.

Exactly how these submicron fragments interact with the surrounding Mn–Fe varnish can be seen in HRTEM imagery (Fig. 16). The lamellate fabric of the varnish appears to fold around detrital grains. Thus, once the grain reaches its preferred orientation somewhat parallel with the fabric, varnish continues to grow over and around the mineral dust.

### 4.3. Heterogeneity of dust assemblages within layers

Many varnishes contain zones enriched in detrital grains sandwiched between layered varnish with lower concentrations of

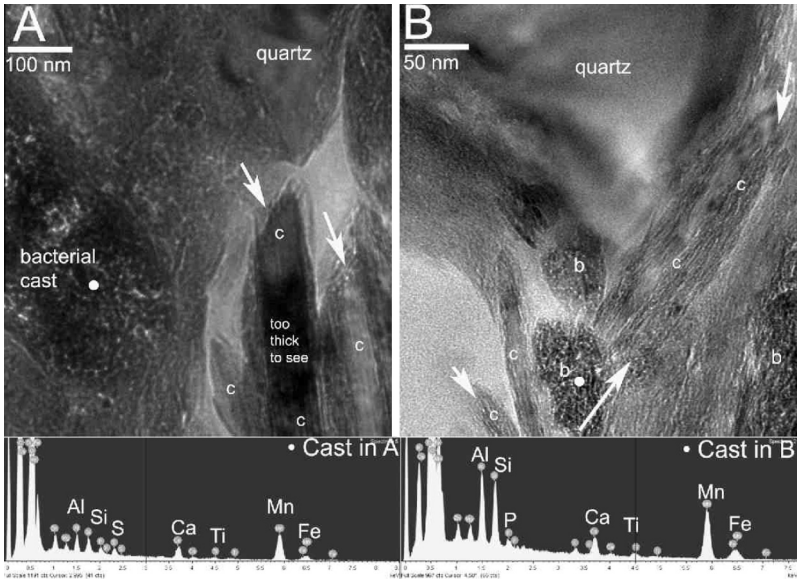


**Fig. 9.** Quartz mineral grains enveloped by varnish collected from Death Valley. The varnish includes different basic textures: fragments of bacterial casts (b) that have a granular texture possibly derived through ongoing decay of the bacterial casts (Krinsley, 1998) and clay minerals pods (c) that show some evidence of weathering along the edges (Robert and Tessier, 1992) that have incorporated granules (arrows). The granular texture that is found in contact with the quartz mineral is diagnostic of Mn–Fe-rich bacterial casts – as revealed by EDX analyses at the indicated white dots.

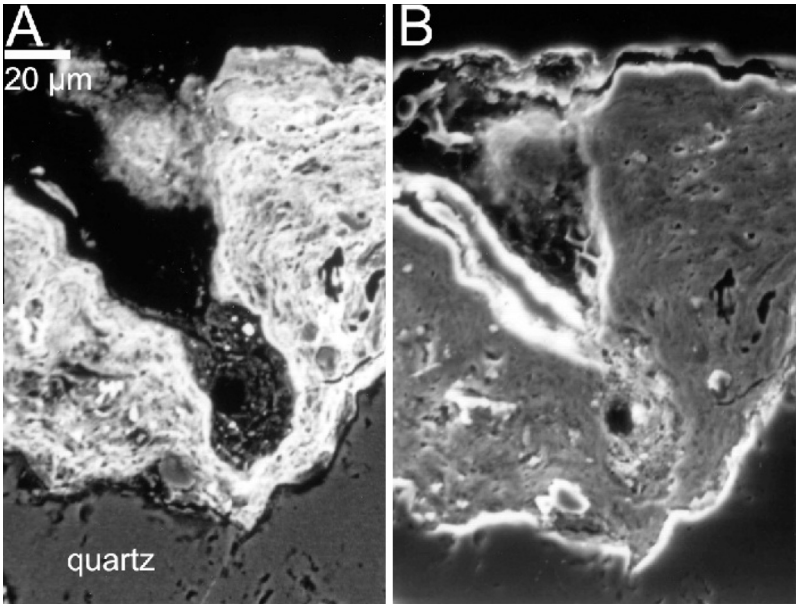


**Fig. 10.** Rock varnish from Panaramittee South Australia imaged with back-scattered (A) and secondary (B) electrons. Microcolonial fungi, known as an agent of active varnish dissolution in Australian deserts (Dragovich, 1993), has eroded a tube into this varnish. The fungi is visible in secondary electrons. (B) Quartz silt has accumulated in the bottom of this tube.

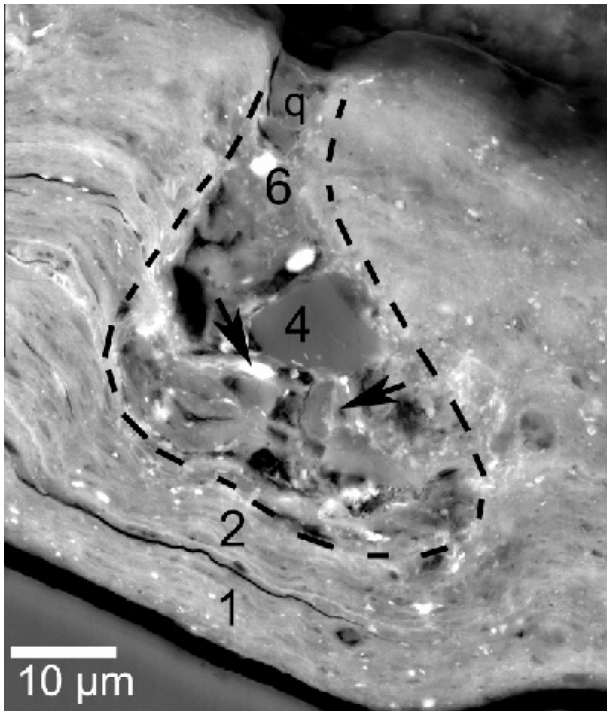


**Fig. 11.** Rock varnish from the Phoenix Mountains, Arizona, illustrates how mineral detritus can become enveloped in a varnish depression. We interpret the sequence as follows: (1) deposition of laminar varnish on the underlying plagioclase (2) continued accretion of laminated varnish; (3) a depression developed into the varnish surface (dashed lines); (4) mineral fragments collected in the depression, including the plagioclase and smaller quartz and magnetite grains; (5) varnish material grew at contact points between the mineral detritus, perhaps from reprecipitation of dissolved varnish material (arrows); and (6) varnish accretion almost completely sealed off the depression, except for a quartz (q) fragment at the top of the tube.

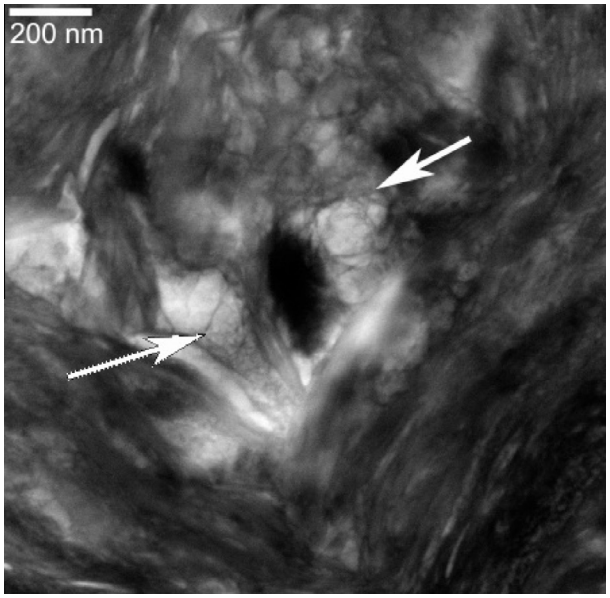


**Fig. 12.** Paleo-depression in rock varnish from Death Valley that was filled by mineral detritus with an irregular surface microtopography (arrows), imaged with SEM. It is possible that the etched surface of this Fe-rich grain (possibly magnetite) aided in its adherence to varnish.

dust. Several different potential explanations of this uneven distribution exist. One mechanism, previously discussed, is deposition of detrital grains in surficial depressions (e.g. Figs. 10 and 11). These depressions are then sealed (Fig. 11). When observed in the middle of a cross-section, these filled depressions appear as pockets of micron-sized mineral detritus mixed with varnish (Fig. 17).

Sometimes, however, the mineral detritus trapped in surface depressions can reach diameters in the range of 10 μm (Fig. 18). While such large sizes are unusual, they do occur and most often in desert pavements. For example, the largest detrital grain in Fig. 18C is sandwiched between two microstromatolite forms and then sealed by layered varnish. Such a particle could have been transported through the action of rainsplash (Furbish et al., 2009). These larger detrital grains often have zones of greater porosity

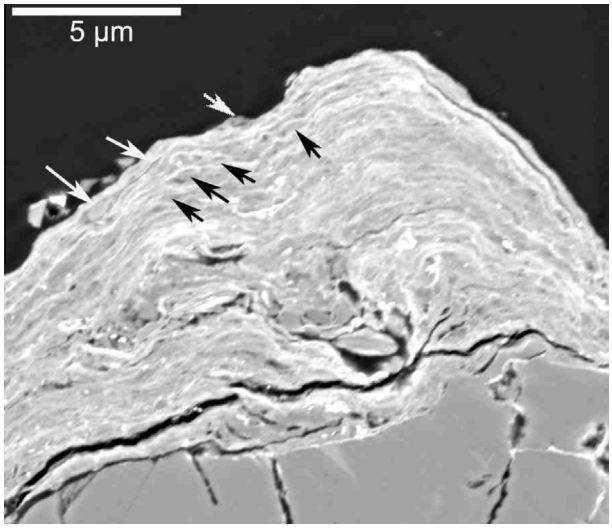


**Fig. 13.** BSE image of rock varnish formed at the Cima Volcanic Field, Mojave Desert. Arrows identify a few of the submicron fragments of quartz resting conformably along varnish laminae with a subparallel orientation.

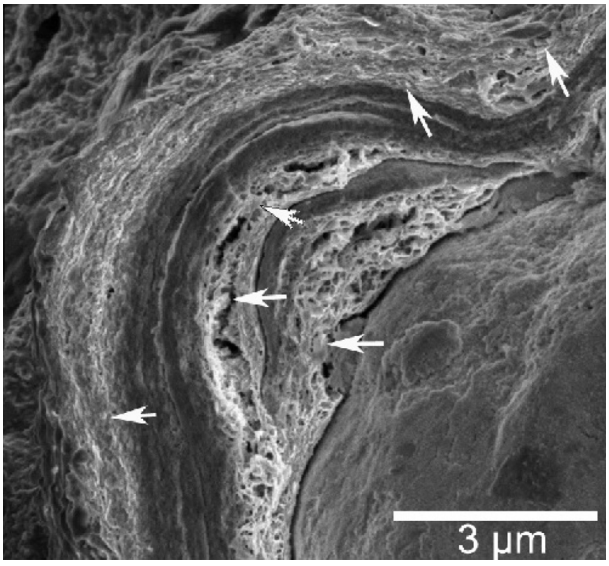


**Fig. 14.** SE image of rock varnish formed at along the Erie Canal, New York. Arrows identify a few of the detrital grains that are submicron in size and orient parallel to the laminations.

surrounding their margins (Fig. 18), perhaps related to the flow of capillary water that remobilizes the varnish that originally entombed the grains.

Heterogeneities in mineral detritus concentration do sometimes occur in a microstratigraphic sequence, where detrital-rich layers alternate with detrital-poor layers. This type of layering is rare, and it is not related to the varnish microlamination research of Tanzhuo Liu (Dorn, 2009b; Liu and Broecker, 2007, 2008a,b). We have only seen it in particularly dusty locations – such as central Arizona (Fig. 19A) with its summer haboobs (Marcus and Brazel, 1992) and the Ashikule Basin (Fig. 19B), Tibet, with its large playa (Krinsley et al., 2009; Wang et al., 2011). We speculate that the alternating layers of laminated and detrital-rich layers reflect alternating periods of low and high dust storm activity. If this speculation is correct, the tendency to form laminated varnish could be overwhelmed periodically during dusty intervals.

Yet another possibility for some of the observed heterogeneities in mineral detritus could be differential leaching (Dorn and Krinsley, 1991). Note that visual abundance of micron-sized quartz detritus in Fig. 20 occurs in the area of greatest varnish porosity. The micron-sized quartz appears to have an oval shape with a long axis semi-parallel to the texture of the varnish. These same sized grains occur in adjacent varnish, but leaching makes it easier to see quartz grains when surrounded by pores.

### 4.4. Evaluating potential influences of dust mineralogy on varnish

The information we have on the mineralogy of the aeolian mineral dust in observed varnishes (Table 1) comes from EDX spectra that provides insight into elemental abundance (Table 2). Hence, the detrital grain mineralogy discussed in this section is only inferred. For example, seeing peaks of just Si and O for a spot analysis infers a quartz (or amorphous silica) mineralogy, especially if the BSE texture is homogenous. Seeing a peak of just Fe would indicate some iron oxide/hydroxide, and so forth for plagioclase, orthoclase, and other rock-forming minerals enveloped by varnish.

Taken as a whole, quartz is – by far – the most commonly observed dust mineral incorporated into varnish (e.g. Figs. 5–11, 13–16, 18 and 20). The second most commonly observed grain is iron oxide/hydroxide, perhaps magnetite (e.g. Figs. 12, 16, 17, 18D, 19). While other common minerals like feldspars are sometimes seen (e.g. Figs. 18 and 19), the disproportional representation of quartz seen in the observed varnishes could have several explanations.

Accreting manganese oxides such as varnish tends to grow very slowly over a smooth quartz surface, but incipient varnish tends to nucleate and spread faster over a feldspar surface (Dorn and

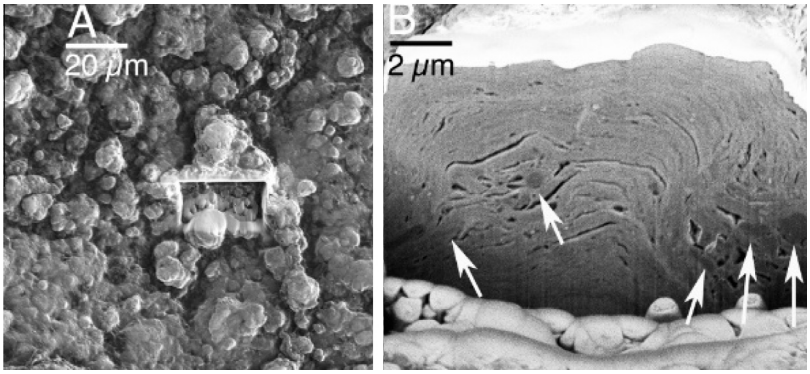


**Fig. 15.** Stromatolitic (botryoidal) textured varnish, imaged in A, collected at the surface of Yucca Mountain, Nevada contains submicron gray quartz particles identified by arrows in the DB-FIB sectioning in B. The oval forms at the bottom of image B and the bright material at the top are artifacts of FIB preparation.

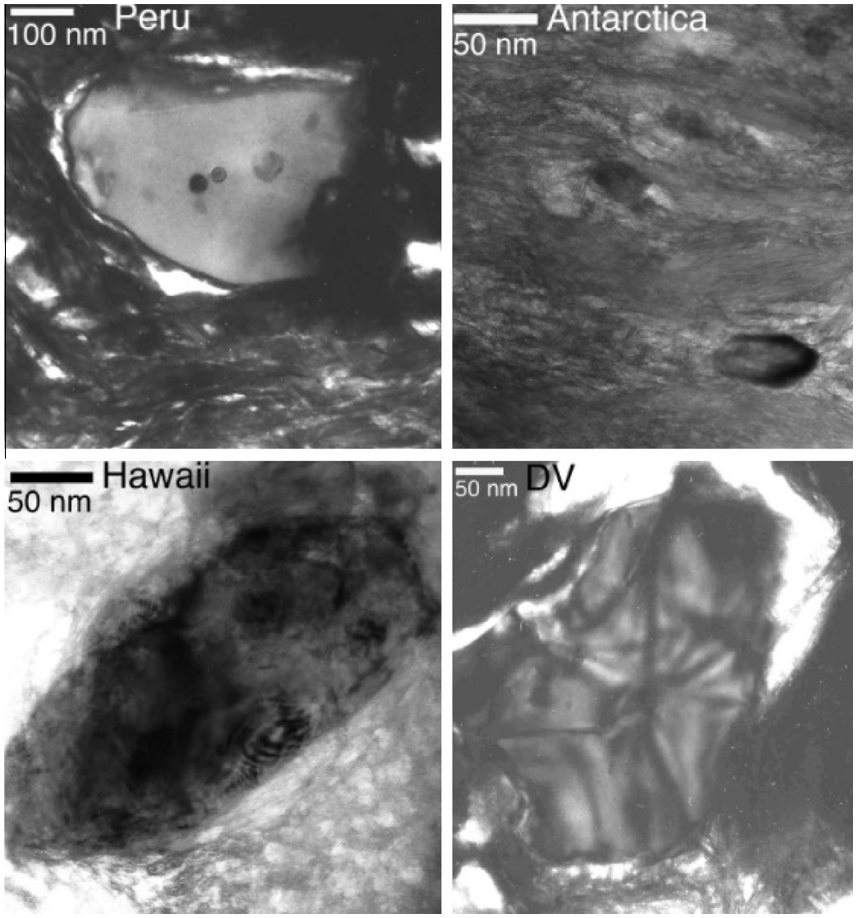


**Fig. 16.** HRTEM images of detrital grains in varnishes from different global settings: quartz in varnish from Nasca, Peru; quartz in varnish from Antarctica; magnetite from Hawai'i; and barite from Death Valley, CA. Mineral identification is based on EDX analyses.

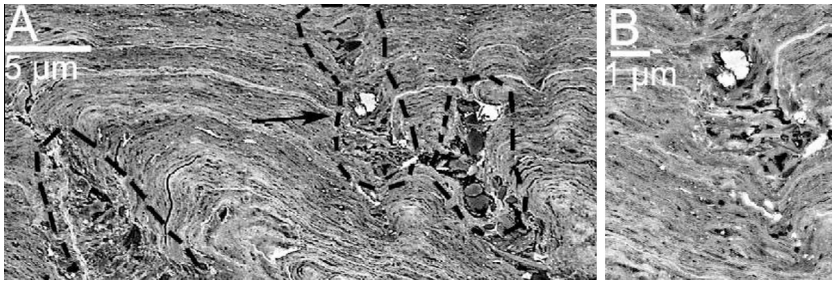


**Fig. 17.** BSE image of varnish cross-section from a bedrock outcrop, near Alice Springs, Australia. Micron-sized mineral detritus accumulated in what were once depressions eroded into the laminated varnish – as evidenced by the truncation of some of the microlaminae. Image A shows several microdepressions identified by dashed lines. The arrow in image A identifies the location of image B, a former depression sealed by layered varnish. The left-most filled depression in image A shows redeposition of mobilized Mn and Fe in the form of a bright Mn–Fe-rich stringer – as reported elsewhere (Garvie et al., 2008; Krinsley et al., 1990).

Oberlander, 1982). Thus, we think it unlikely that quartz minerals would be preferentially adsorbed into varnish.

However, quartz has long been recognized as being prevalent in aeolian dust (McTainsh et al., 2013; Pye, 1987), and this prevalence could be reflected in what is enveloped in varnish.

The relative lack of minerals such as feldspars and amphiboles could also have to do with their susceptibility to decay into clay minerals, especially if the particles are small with a high surface area. Common weathering products such as gibbsite and kaolinite are formed through the dissolution of feldspar. Thus, we speculate that the relative paucity of rock-forming minerals that decay into clays could be due in part to *in situ* diagenesis. The process of *in situ* decay of feldspar starts at the micron scale, as seen in Fig. 21; a detrital grain falls into a varnish depression and begins to decay on the edges. Eventually, we speculate, it turns to clay *in situ*, as seen at the nanoscale in the HRTEM image in Fig. 21. Then, the Mn-rich bacterial cast granules move into the ragged edges of the clay mineral.

An uncertain issue with the polygenetic model of varnish formation (Fig. 2D) involves the role of water in transporting the Mn-encrusted cast pieces of bacteria into the feathered edges of clay minerals. Wetting events must dissolve the nanometer-scale fragments, but the process of water movement through tightly laminated clay minerals remains unexplained. Consider Fig. 9

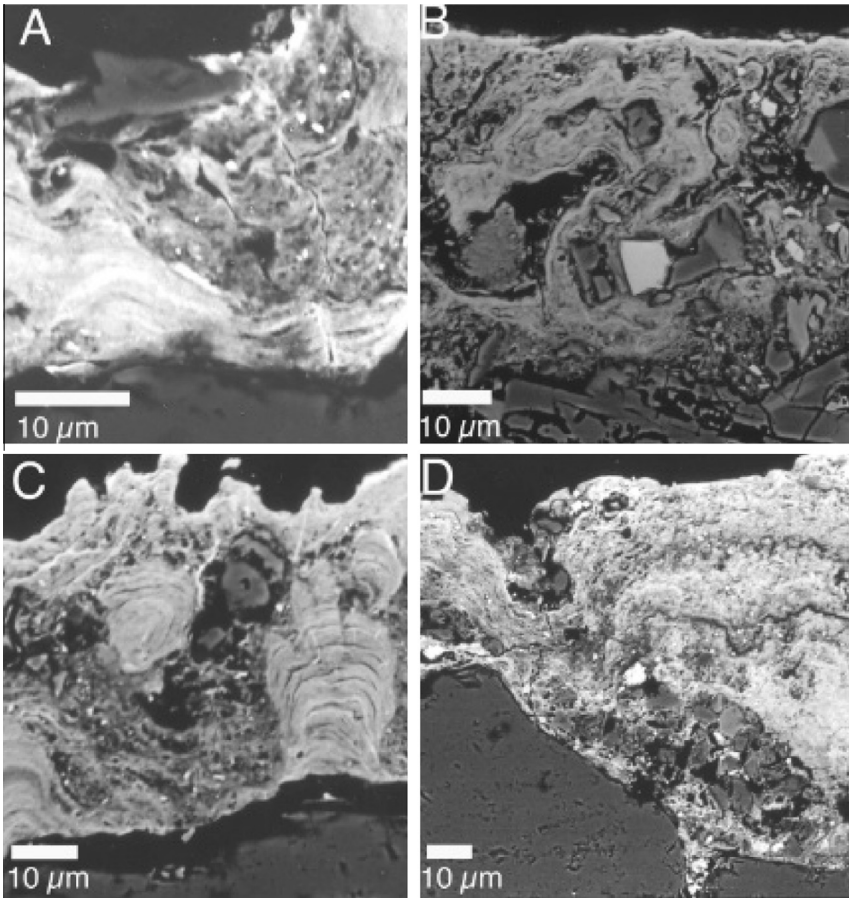


**Fig. 18.** BSE images of varnish cross-sections that contain detrital minerals in the range of 10 μm, where EDX was used to infer mineralogy. (A) Desert pavement at Nazca, Peru where the large detrital grain is quartz. (B) Tunisia varnish sample collected by N. Drake (Drake et al., 1993) where the darker detrital grains are quartz and the brighter grains are orthoclase. (C) Desert pavement, Negev Desert where the larger detrital grains are quartz. (D) Desert pavement on an alluvial fan, near Marsa Muqualba, Sinai Peninsula, Egypt where the detrital grains are mostly quartz, but magnetite and orthoclase also occur.

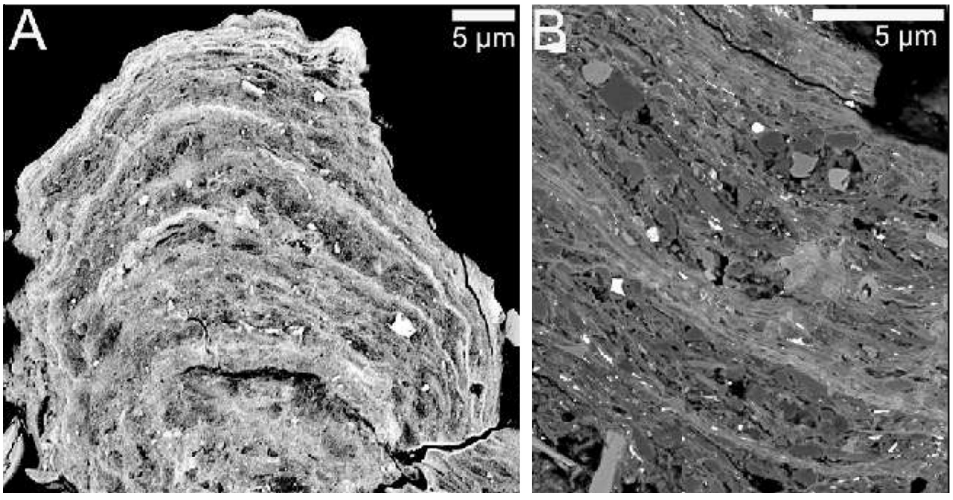


**Fig. 19.** BSE images of varnishes from the Phoenix Mountains, Sonoran Desert, and the Ashikule Basin, Tibet. In both locations, laminated varnish alternates with detritus-rich layers.

where the granular-textured remains of bacteria casts have moved a few nanometers into layered clays.

There exist minimal pore space and low interconnectivity of pores throughout layered clays, intuitively reducing the capacity for water transport throughout these materials. Water able to flow through micro- or nano-scale fractures within clay laminations is unlikely to penetrate these laminations deeply. This water has the potential to be adsorbed on clay surfaces or incorporated into momentary hydration, precluding too much penetration into the laminations. Additionally, layered clays are tightly bound due to

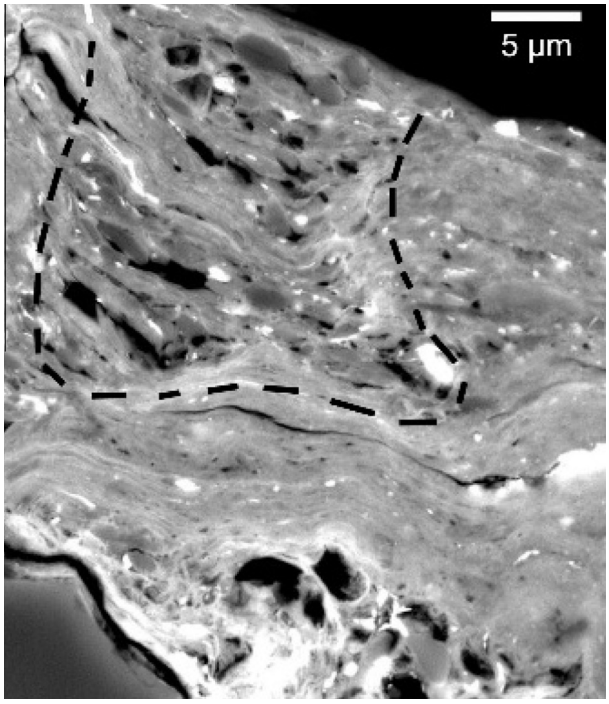


**Fig. 20.** Quartz silt is more apparent in varnish from a desert pavement near Florence, Arizona, in a zone of greater porosity. The dashed black lines outline a texture that is associated with a zone where intense cation leaching produced micron-scale pores (Dorn and Krinsley, 1991).

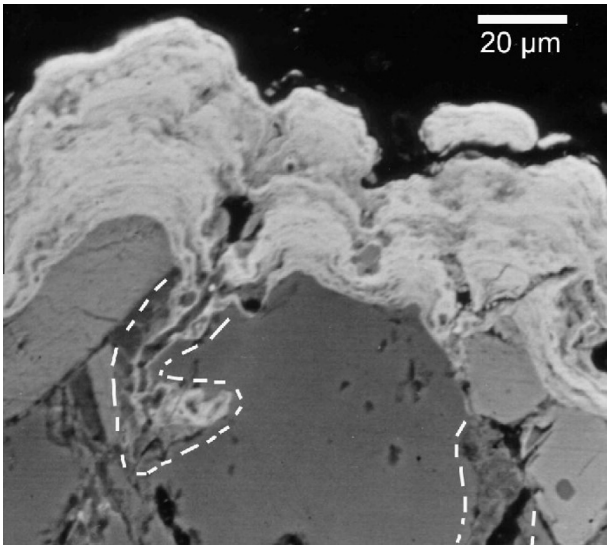


**Fig. 22.** BSE image of varnish accretion near the summit of Kitt Peak, Arizona. Even as varnishing progresses the underlying minerals decay, generating pore spaces. Dissolution of subjacent minerals proceeds as remobilization of varnish constituents find their way into the underlying pore spaces (dashed zones). The textures of these areas of redeposited varnish are chaotic, reflecting ongoing diagenesis with bright areas of Mn and Fe, and gray areas with more Si and Al, as indicated by EDX analyses.

their maximal surface area contacts with adjacent layers. Thus, precipitated minerals such as iron and manganese oxides are typically found in the immediate clay lamination structures in the vicinity of granular bacterial casts or areas of enhanced porosity. Strong laminated appearance is resumed further away from these regions of enhanced porosity created by bacterial casts, collections of detrital grains, or natural fractures in the rock coating.

Detrital minerals offer one mechanism to explain water transport through tightly laminated varnish. The FIB sample preparation process preserved the nanoscale topography of a Fe-rich detrital grain imaged in Fig. 12. Note the irregular etched-like surface of the grain. Minerals like quartz and magnetite undergo thermal expansion and contraction. For example, thermal expansion can occur when quartz exhibits anisotropic behavior where one axis contracts with heating while the others expand (Luque et al., 2011) as much as ~20% (de Castro Lima and Paraguassú, 2004). With wetting (and associated cooling in a desert) and drying (and associated heating in a desert), it is possible that the sides of these expanding and contracting detrital minerals provide a conduit for capillary water transport. This hypothesis could explain the enhanced porosity at nanometer-scale around the mineral grains presented in Fig. 16. Continued capillary water transport would then enhance these pore spaces, leading to the condition

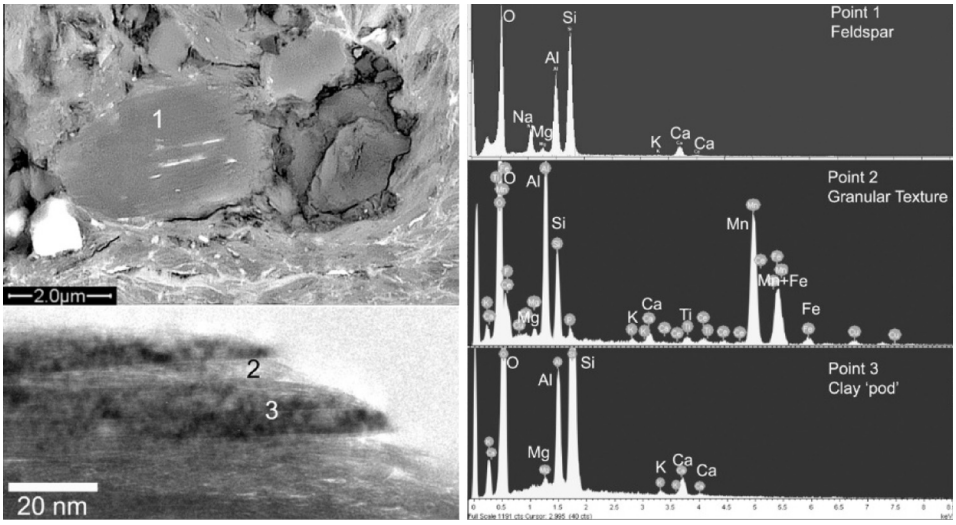


**Fig. 21.** The *in situ* decay of feldspar (as indicated by EDX Point 1), seen in the upper left BSE image, starts with deposition in a depression on the varnish surface. Note how the edges have a ragged appearance – indicating ongoing decay probably through discongruent dissolution. Deeper in this same varnish from near Florence, Arizona, a "pod" of a clay mineral (EDX Point 3) is imaged through HRTEM. Given its chemistry, it could have derived ultimately from *in situ* decay of feldspar mineral dust. The next stage in decay results when the granular-textured remains of a bacterial cast (EDX Point 2) precipitates inside the ragged edges of clay minerals. The granular source of the Mn-rich granular material is directly underneath the clay pod.

seen in Figs. 11, 17, 18 and 20, where the greatest zones of porosity are adjacent to these detrital mineral grains.

A broader implication of the aeolian mineral dust enveloped into varnish is an antipathy with the varnish microlamination (VML) technique (Liu, 2013; Liu and Broecker, 2007, 2008a,b, 2013). The evidence presented here makes it clear that the presence of irregularly-shaped mineral grains enhances post-depositional modification of varnish. Since the VML method relies on preserving a paleoclimatic record embedded in the geochemistry of the synsedimentary deposit, any post depositional modification destroys this record. This research, thus, provides confirming support for the general VML sampling strategy of avoiding microenvironments that would favor contact with aeolian mineral dust (Dorn, 2009b; Liu, 2003).

### 4.5. Mineral-varnish interactions at the base

For the first 170 years of varnish research, starting with von Humbolt's (1812) observations – the consensus of scientific opinion was that varnish derives from solutes leached out of the underlying rock (Bard et al., 1978; Birot, 1969; Blake, 1905; Engel and Sharp, 1958; Glennie, 1970; Holmes, 1965; Hume, 1925; Hunt, 1954; Linck, 1901, 1928; Longwell et al., 1950; Lucas, 1905; Marshall, 1962; Merrill, 1898; Peel, 1960; Walther, 1891; Wilhelmy, 1964; Woolnough, 1930). The host rock was the perceived key to varnish formation, where solutions of decayed minerals migrated outward to form varnish. It is perhaps ironic that our imagery of mineral-varnish interactions reveals that it is the varnish that invades the underlying rock.

Microscopic examination of very base of rock varnish suggests that rock varnish can be more stable in the subaerial geochemical environment than the underlying rock minerals. Consider Fig. 22, where the remobilized products of rock varnish are deposited in pore spaces created by dissolution of the underlying rock minerals. Thus, even though varnish often experiences dissolution, the net accretion of new varnish produces a condition where redeposited varnish constituents impregnate the weathering rind of the underlying rock.

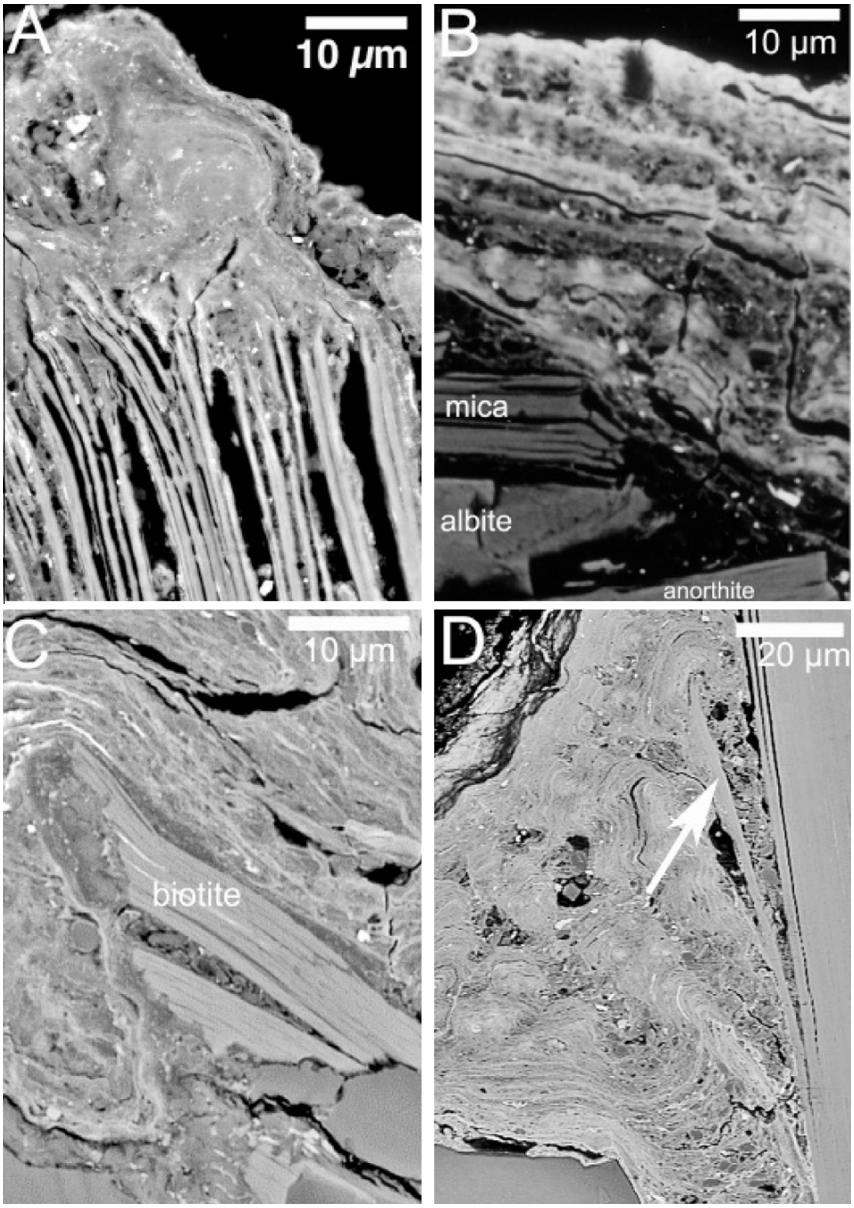


**Fig. 23.** Interactions of rock varnish with the pore spaces of the underlying rock. (A) Varnish migrating into biotite, Ashikule Basin, Tibet. (B) Varnish collapsing into porosity of the underlying rock, cataracts of the Orinoco River, Venezuela. (C) Varnish infilling biotite, Phoenix Mountains, Arizona. (D) Varnish moving into biotite (arrow), as it splits apart, desert pavement, Florence, Arizona.

The net effect of ongoing decay of host rock minerals, ongoing accretion of rock varnish, and ongoing mobilization of varnish constituents into the pore spaces of minerals in the underlying rock is gradual replacement of outermost sections of underlying rock with redeposited varnish (Fig. 23). The process of the gradual migration of varnish and other types of rock coatings into the underlying rock results in the geomorphic phenomenon of case hardening (Dorn et al., 2012a).

## 5. Conclusion

Analyses of samples from 19 different field sites scattered over five continents and employing a mix of electron microscope techniques reveals that aeolian mineral dust influences rock varnish development. While most of the mineral grains that come to rest on varnish are not incorporated, nanoscale manganese–iron laminations envelope some grains and weakly adhere them to varnish surfaces. In this initial phase, the nanoscale of the attaching varnish appears quite fragile; small shear stresses from rainsplash and overland flow could result in detachment. Eventually, however, further deposition of laminated varnish embeds some of the mineral particles.

Most detrital particles appear to have an oval shape and come to rest conformably between accreting laminated varnish. Some detrital particles, though, are trapped in deeper depressions some of which are formed by acid-producing lithobionts such as lichens and microcolonial fungi. In circumstances where dust is particularly prevalent in the environment, layering of detrital-rich and detrital-poor laminae occurs – perhaps reflecting alternating period of low and high dust storm activity. Such layering is rare and is unrelated to the varnish microlaminations used in paleoclimatic research (Liu and Broecker, 2007, 2008a,b).

Quartz dominates the mineralogy of aeolian dust enveloped into varnish. In contrast, feldspars are rarely seen; this may be from *in situ* diagenesis that alters feldspares into some of the observed clay minerals. Detrital aeolian mineral grains appear to enhance water movement at the nanoscale, facilitating movement of Mn-rich bacterial cast remains into clay minerals. The enhancement of water transport around the margins of detrital grains promotes post depositional mobility of Mn–Fe oxides. The capillary water flowing through these larger pores transports manganese and iron that can be deposited around detrital minerals and in fractures as stringers. This is consistent with varnish microlamination method not working well in samples that accumulate aeolian mineral grains.

All of the mineral dust particles found at the top of varnish and within varnish derive from external sources. The external source could be dust deflated from thousands of kilometers away or a mineral detached from an exposed rock a few millimeters distant. However, at the base of the varnish, minerals in the underlying rock do sometimes mix with varnish. This mixing occurs when ongoing decay in the underlying rock minerals open up pore spaces. Mobilized varnish then deposits inside these pore spaces.

## Acknowledgments

We thank Steve Gordon for assistance in generating the chemical maps, Alice Tratebas and the BLM for permission to work with the Whoopup sample, N. Drake for sending the Tunisia sample, Barry DiGregorio for sending samples from New York, Margaret Nobbs for help in obtaining the permissions to sample Panaramittee rock art, and two hard-working reviewers for their efforts in improving the manuscript.

## References

Allen, C., Probst, L.W., Flood, B.E., Longazo, T.G., Scheble, R.T., Westall, F., 2004. Meridiani Planum hematite deposit and the search for evidence of life on Mars – iron mineralization of microorganisms in rock varnish. Icarus 171, 20–30.
Baker, V.R., Bunker, R.C., 1985. Cataclysmic late Pleistocene flooding from glacial Lake Missoula: a review. Quatern. Sci. Rev. 41, 1–41.
Bard, J.C., Asaro, F., Heizer, R.F., 1978. Perspectives on the dating of prehistoric Great Basin petroglyphs by neutron activation analysis. Archaeometry 20, 85–88.
Basedow, H., 1914. Aboriginal rock carvings of great antiquity in South Australia. J. Roy. Anthropol. Inst. 44, 195–211.
Birot, P., 1969. The Cycle of Erosion in Different Climates. University of California Press, Berkeley.
Bishop, J.L., Murchie, S.L., Pieters, C.M., Zent, A.P., 2002. A model for formation of dust, soil, and rock coatings on Mars: physical and chemical processes on the Martian surface. J. Geophys. Res. 107 (E11). http://dx.doi.org/10.1029/2001JE001581.
Blake, W.P., 1905. Superficial blackening and discoloration of rocks especially in desert regions. Trans. Am. Inst. Min. Eng. 35, 371–375.
Bretz, J.H., 1923. The channeled scabland of the Columbia Pleateau. J. Geol. 31, 617–649.
Brook, G.A., Railsback, L.B., Campbell, A.C., Robbins, L.H., Murphy, M.L., Hodgins, G., McHugh, J., 2011. Radiocarbon ages for coatings on cupules ground in quartzite bedrock at Rhino Cave in the Kalahari Desert of Botswana, and their paleoclimatic significance. Geoarchaeology 26, 61–82.
Brown, D.J., Lee, M.R., 2007. From microscopic minerals to global climate change? Geol. Today 23 (5), 172–177.
Conca, J., 1982. Case hardening of the surface features: Earth analogs to the Martian surface. Lunar Planet. Sci. 13, 125–126.
Conca, J.L., Rossman, G.R., 1982. Case hardening of sandstone. Geology 10, 520–525.
de Castro Lima, J.J., Paraguassú, A.B., 2004. Linear thermal expansion of granitic rocks: influence of apparent porosity, grain size and quartz content. Bull. Eng. Geol. Environ. 63, 215–220.
Ditto, J., Krinsley, D., Langworthy, K., 2012. Localized grounding, excavation, and dissection using in-situ probe techniques for focused ion beam and scanning electron microscopy: experiments with rock varnish. Scanning 34, 279–283.
Dorn, R.I., 1986. Rock varnish as an indicator of aeolian environmental change. In: Nickling, W.G. (Ed.), Aeolian Geomorphology. Allen & Unwin, London, pp. 291–307.
Dorn, R.I., 1998. Rock Coatings. Elsevier, Amsterdam.
Dorn, R.I., 2007a. Baking black opal in the desert sun: the importance of silica in desert varnish (COMMENT). Geology. http://dx.doi.org/10.1130/G23410C.1.
Dorn, R.I., 2007b. Rock varnish. In: Nash, D.J., McLaren, S.J. (Eds.), Geochemical Sediments and Landscapes. Blackwell, London, pp. 246–297.
Dorn, R.I., 2009a. Desert rock coatings. In: Parsons, A.J., Abrahams, A. (Eds.), Geomorphology of Desert Environments. Springer, Amsterdam, pp. 153–186.
Dorn, R.I., 2009b. The rock varnish revolution: new insights from microlaminations and the contribution of Tanzhuo Liu. Geogr. Compass 3, 1804–1823.
Dorn, R.I., DeNiro, M.J., 1985. Stable carbon isotope ratios of rock varnish organic matter: a new paleoenvironmental indicator. Science 227, 1472–1474.
Dorn, R.I., Dorn, J., Harrison, E., Gutbrod, E., Gibson, S., Larson, P., Cerveny, N., Lopat, N., Groom, K.M., Allen, C.D., 2012a. Case hardening vignettes from the western USA: convergence of form as a result of divergent hardening processes. Assoc. Pacific Coast Geogr. Yearbook 74, 1–12.
Dorn, R.I., Gordon, M., Pagán, E.O., Bostwick, T.W., King, M., Ostapuk, P., 2012b. Assessing early Spanish explorer routes through authentication of rock inscriptions. Prof. Geogr. 64, 415–429.
Dorn, R.I., Krinsley, D.H., 1991. Cation-leaching sites in rock varnish. Geology 19, 1077–1080.
Dorn, R.I., Krinsley, D.H., 2011. Spatial, temporal and geographic considerations of the problem of rock varnish diagenesis. Geomorphology 130, 91–99.
Dorn, R.I., Krinsley, D.H., Ditto, J., 2012c. Alexander von Humbodlt's initiation of rock coating research. J. Geol. 120, 1–12.
Dorn, R.I., Krinsley, D.H., Liu, T., Anderson, S., Clark, J., Cahill, T.A., Gill, T.E., 1992. Manganese-rich rock varnish does occur in Antarctica. Chem. Geol. 99, 289–298.
Dorn, R.I., Meek, N., 1995. Rapid formation of rock varnish and other rock coatings on slag deposits near Fontana. Earth Surf. Proc. Land. 20, 547–560.
Dorn, R.I., Oberlander, T.M., 1981. Microbial origin of desert varnish. Science 213, 1245–1247.
Dorn, R.I., Oberlander, T.M., 1982. Rock varnish. Prog. Phys. Geogr. 6, 317–367.
Dragovich, D., 1986. Weathering of desert varnish by lichens. In: 21st I.A.G. Proceedings, pp. 407–412.
Dragovich, D., 1987. Weathering of desert varnish by lichens. In: Conacher, A. (Ed.), Readings in Australian Geography. Proceedings of the 21st IAG Conference, Perth, pp. 407–412.
Dragovich, D., 1993. Distribution and chemical composition of microcolonial fungi and rock coatings from arid Australia. Phys. Geogr. 14, 323–341.
Drake, N.A., Heydeman, M.T., White, K.H., 1993. Distribution and formation of rock varnish in southern Tunisia. Earth Surf. Proc. Land. 18, 31–41.
Engel, C.G., Sharp, R.S., 1958. Chemical data on desert varnish. Geol. Soc. Am. Bull. 69, 487–518.
Etienne, S., 2002. The role of biological weathering in periglacial areas: a study of weathering rinds in south Iceland. Geomorphology 47, 75–86.
Fabero-Longo, S.E., Gazzano, C., Girlanda, M., Castelli, D., Tretiach, M., Baiocchi, C., Piervittori, R., 2011. Physical and chemical deterioration of silicate and carbonate rocks by meristematic microcolonial fungi and endolithic lichens (Chaetothryiomycetidae). Geomicrobiol. J. 28, 732–744.

Francis, W.D., 1921. The origin of black coatings of iron and manganese oxides on rocks. Proc. Roy. Soc. Queensland 32, 110–116.
Furbish, D.J., Childs, E.M., Haff, P.K., Schmeeckle, M.W., 2009. Rain splash of soil grains as a stochastic advection–dispersion process, with implications for desert plant–soil interactions and land-surface evolution. J. Geophys. Res. 114, F00A03. http://dx.doi.org/10.1029/2009JF001265, 18p.
Gadd, G.M., 2007. Geomycrology: biogeochemical transformations of rocks, minerals, metals and radionuclides by fungi, bioweathering and bioremediation. Mycol. Res. 111, 3–49.
Ganor, E., Kronfeld, J., Feldman, H.R., Rosenfeld, A., Ilani, S., 2009. Environmental dust: a tool to study the patina of ancient artifacts. J. Arid Environ. 73, 1170–1176.
Garvie, L.A.J., Burt, D.M., Buseck, P.R., 2008. Nanometer-scale complexity, growth, and diagenesis in desert varnish. Geology 36, 215–218.
Glennie, K.W., 1970. Desert Sedimentary Environments. Elsevier, Amsterdam.
Goldstein, J., Newbury, D.E., Joy, D.C., Lyman, C.E., Echlin, P., Lifshin, E., Sawyer, T.L., Michael, J.R., 2003. Scanning Electron Microscopy and X-Ray Microanalysis. Elsevier, Amsterdam.
Gorbushina, A.A., 2003. Microcolonial fungi: survival potential of terrestrial vegetative structures. Astrobiology 3, 543–554.
Gorbushina, A.A., 2007. Life on the rocks. Environ. Microbiol. 9, 1613–1631.
Gordon, S.J., Dorn, R.I., 2005. In situ weathering rind erosion. Geomorphology 67, 97–113.
Grote, G., Krumbein, W.E., 1992. Microbial precipitation of manganese by bacteria and fungi from desert rock and rock varnish. Geomicrobiology 10, 49–57.
Haberland, W., 1975. Untersuchungen an Krusten, Wustenlacken und Polituren auf Gesteinsoberflachen der nordlichen und mittlerent Saharan (Libyen und Tchad). Berl. Geogr. Abh. 21, 1–77.
Harrington, C.D., 1988. Recognition of components of volcanic ash in rock varnish and the dating of volcanic ejecta plumes. Geol. Soc. Am. Abstr. Programs 20, 167.
Hirsch, P., Eckhardt, F.E.W., Palmer, R.J., 1995. Methods for the study of rock-inhabiting microorganisms – a mini review. J. Microbiol. Methods 23, 143–167.
Holmes, A., 1965. Principles of Physical Geology. Ronald Press, New York.
Hooke, R.L., Yang, H., Weiblen, P.W., 1969. Desert varnish: an electron probe study. J. Geol. 77, 275–288.
Hume, W.F., 1925. Geology of Egypt. The Surface Features of Egypt, Their Determining Causes and Relation to Geologic Structure, vol. 1. Government Press, Cairo.
Hungate, B., Danin, A., Pellerin, N.B., Stemmler, J., Kjellander, P., Adams, J.B., Staley, J.T., 1987. Characterization of manganese-oxidizing (MnII → MnIV) bacteria from Negev Desert rock varnish: implications in desert varnish formation. Can. J. Microbiol. 33, 939–943.
Hunt, C.B., 1954. Desert varnish. Science 120, 183–184.
Jordan, D.W., 1954. The adhesion of dust particles. Br. J. Appl. Phys. 5, S194–S198.
Khalaf, F.I., AlShubaibi, A.A., 2012. Occurrence and characteristics of Quaternary calcareous microbialitic crust in the southern desert of Kuwait, Arabian Gulf. J. Arid Environ. 79, 48–55.
Klute, F., Krasser, L.M., 1940. Über wüstenlackbildung im Hochgebirge. Petermanns Geogr. Mitt. 86, 21–22.
Krinsley, D., 1998. Models of rock varnish formation constrained by high resolution transmission electron microscopy. Sedimentology 45, 711–725.
Krinsley, D., Dorn, R.I., Anderson, S., 1990. Factors that may interfere with the dating of rock varnish. Phys. Geogr. 11, 97–119.
Krinsley, D., Dorn, R.I., DiGregorio, B.E., 2009. Astrobiological implications of rock varnish in Tibet. Astrobiology 9, 551–562.
Krinsley, D., Rusk, B.G., 2000. Bacterial presence in layered rock varnish – possible Mars analog? Mars Polar Sci. 2000, 4001.pdf.
Krinsley, D.H., Dorn, R.I., DiGregorio, B.E., Langworthy, K.A., Ditto, J., 2012. Rock varnish in New York: an accelerated snapshot of accretionary processes. Geomorphology 138, 339–351.
Krinsley, D.H., Dorn, R.I., Tovey, N.K., 1995. Nanometer-scale layering in rock varnish: implications for genesis and paleoenvironmental interpretation. J. Geol. 103, 106–113.
Krumbein, W.E., 1969. Über den Einfluss der Mikroflora auf die Exogene Dynamik (Verwitterung und Krustenbildung). Geol. Rundsch. 58, 333–363.
Kuhlman, K.R., Fusco, W.G., La Duc, M.T., Allenbach, L.B., Ball, C.L., Kuhlman, G.M., Anderson, R.C., Erickson, K., Stuecker, T., Benardini, J., Strap, J.L., Crawford, R.L., 2006. Diversity of microorganisms within rock varnish in the Whipple Mountains, California. Appl. Environ. Microbiol. 72, 1708–1715.
Langworthy, K., Krinsley, D., Dorn, R.I., 2010. High resolution transmission electron microscopy evaluation of silica glaze reveals new textures. Earth Surf. Proc. Land. 35, 1615–1620.
Linck, G., 1901. Über die dunkelen Rinden der Gesteine der Wüste. Jenaische Z. Naturwissenschaft 35, 329–336.
Linck, G., 1928. Über Schutzrinden. Chem. Erde 4, 67–79.
Liu, T., 2003. Blind testing of rock varnish microstratigraphy as a chronometric indicator: results on late Quaternary lava flows in the Mojave Desert, California. Geomorphology 53, 209–234.
Liu, T., 2013. VML Dating Lab. <http://www.vmldating.com/> (last accessed 28.02.13).
Liu, T., Broecker, W.S., 2000. How fast does rock varnish grow? Geology 28, 183–186.
Liu, T., Broecker, W.S., 2007. Holocene rock varnish microstratigraphy and its chronometric application in drylands of western USA. Geomorphology 84, 1–21.
Liu, T., Broecker, W.S., 2008a. Rock varnish evidence for latest Pleistocene millennial-scale wet events in the drylands of western United States. Geology 36, 403–406.
Liu, T., Broecker, W.S., 2008b. Rock varnish microlamination dating of late Quaternary geomorphic features in the drylands of the western USA. Geomorphology 93, 501–523.
Liu, T., Broecker, W.S., 2013. Millennial-scale varnish microlamination dating of late Pleistocene geomorphic features in the drylands of western USA. Geomorphology. http://dx.doi.org/10.1016/j.geomorph.2012.1012.1034.
Longwell, C.R., Knopf, A., Flint, R.F., 1950. Physical Geology, third ed. Wiley, New York.
Lucas, A., 1905. The blackened rocks of the Nile cataracts and of the Egyptian deserts. National Printing Department, Cairo.
Luque, A., Ruiz-Agudo, E., Cultrone, G., Sebastián, E., Siegsmund, S., 2011. Direct observation of microcrack development in marble caused by thermal weathering. Environ. Earth Sci. 62, 1375–1386.
Mantha, N.M., Schindler, M., Murayama, M., Hochella, M.F., 2012. Silica- and sulfate-bearing rock coatings in smelter areas: products of chemical weathering and atmospheric pollution: I. Formation and mineralogical composition. Geochim. Cosmochim. Acta 85, 254–274.
Marcus, M.G., Brazel, A.J., 1992. Summer dust storms in the Arizona Desert. In: Janelle, D.G. (Ed.), Geographical Snapshots of North America. Guilford Press, New York, pp. 411–415.
Marshall, R.R., 1962. Natural radioactivity and the origin of desert varnish. Trans. Am. Geophys. Union 43, 446–447.
McKeown, D.A., Post, J.E., 2001. Characterization of manganese oxide mineralogy in rock varnish and dendrites using X-ray absorption spectroscopy. Am. Mineral. 86, 701–713.
McTainsh, G., Livingston, I., Strong, C., 2013. Fundamentals of aeolian sediment transport: aeolian sediments. In: Lancaster, N., Sherman, D.J., Baas, A.C.W. (Eds.), Treatise on Geomorphology. Aeolian Geomorphology. Academic Press, San Diego, pp. 23–42.
Merrill, G.P., 1898. Desert varnish. US Geol. Surv. Bull. 150, 389–391.
Northup, D.E., Snider, J.R., Spilde, M.N., Porter, M.L., van de Kamp, J.L., Boston, P.J., Nyberg, A.M., Bargar, J.R., 2010. Diversity of rock varnish bacterial communities from Black Canyon, New Mexico. J. Geophys. Res. 115 (G02007). http://dx.doi.org/10.1029/2009JG001107.
Palmer, F.E., Staley, J.T., Murray, R.G.E., Counsell, T., Adams, J.B., 1985. Identification of manganese-oxidizing bacteria from desert varnish. Geomicrobiol. J. 4, 343–360.
Parchert, K., Spilde, M.N., Porras-Alfaro, A., Nyberg, A.M., Northrup, D.E., 2012. Fungal communities associated with rock varnish in Black Canyon, New Mexico: casual inhabitants or essential partners. Geomicrobiol. J. 29, 752–766.
Peel, R.F., 1960. Some aspects of desert geomorphology. Geography 45, 241–262.
Perry, R.S., Adams, J., 1978. Desert varnish: evidence of cyclic deposition of manganese. Nature 276, 489–491.
Perry, R.S., Engel, M., Botta, O., Staley, J.T., 2003. Amino acid analyses of desert varnish from the Sonoran and Mojave deserts. Geomicrobiol. J. 20, 427–438.
Perry, R.S., Kolb, V.M., 2003. Biological and organic constituents of desert varnish: review and new hypotheses. In: Hoover, R.B., Rozanov, A.Y. (Eds.), Instruments, Methods, and Missions for Astrobiology VII. SPIE, Bellingham, pp. 202–217.
Perry, R.S., Lynne, B.Y., Sephton, M.A., Kolb, V.M., Perry, C.C., Staley, J.T., 2006. Baking black opal in the desert sun: the importance of silica in desert varnish. Geology 34, 537–540.
Perry, R.S., Sephton, M.A., 2007. Reply. Geology. http://dx.doi.org/10.1130/G23663Y.1.
Potter, R.M., 1979. The tetravalent manganese oxides: clarification of their structural variations and relationships and characterization of their occurrence in the terrestrial weathering environment as desert varnish and other manganese oxides. Ph.D. Dissertation. Earth and Planetary Science. California Institute of Technology, Pasadena, p. 245.
Potter, R.M., Rossman, G.R., 1977. Desert varnish: the importance of clay minerals. Science 196, 1446–1448.
Pye, K., 1987. Aeolian Dust and Dust Deposits. Academic Press, London.
Robert, M., Tessier, D., 1992. Incipient weathering: some new concepts on weathering, clay formation and organization. In: Martini, I.P., Chesworth, W. (Eds.), Weathering, Soils & Paleosols. Elsevier, Amsterdam, pp. 71–105.
Sanjurjo-Sánchez, J., 2010. Using microscopic techniques to characterise rock coatings on granitic heritage buildings: an overview. J. Adv. Microsc. Res. 5, 78–85.
Scheffer, F., Meyer, B., Kalk, E., 1963. Biologische ursachen der wüstenlackbildung. Z. Geomorphol. 7, 112–119.
Shao, Y., Wyrwoll, K.H., Chappell, A., Huang, J., Lin, Z., McTainsh, G.H., Mikami, M., Tanaka, T.Y., Wang, X., Yoon, S., 2011. Dust cycle: an emerging core theme in Earth system science. Aeol. Res. 2, 181–204.
Smith, B.J., Whalley, W.B., 1988. A note on the characteristics and possible origins of desert varnishes from southeast Morocco. Earth Surf. Proc. Land. 13, 251–258.
Soleilhavoup, F., 1986. Les surfaces de lart rupestre en plein air: relations avec le milieau biophysique et methodes d'etude. L'Anthropologie (Paris) 90, 743–782.
Spilde, M.N., Melim, L.A., Northrup, D.E., Boston, P.J., 2013. Anthropogenic lead as a tracer for rock varnish growth: implications for rates of formation. Geology 41, 263–266.
Staley, J.T., Jackson, M.J., Palmer, F.E., Adams, J.C., Borns, D.J., Curtiss, B., Taylor-George, S., 1983. Desert varnish coatings and microcolonial fungi on rocks of the

Gibson and Great Victoria Desert, Australia. BMR J. Aust. Geol. Geophys. 8, 83–87.
Tratebas, A.M., Cerveny, N., Dorn, R.I., 2004. The effects of fire on rock art: microscopic evidence reveals the importance of weathering rinds. Phys. Geogr. 25, 313–333.
Turkington, A.V., Paradise, T.R., 2005. Sandstone weathering: a century of research and innovation. Geomorphology 67, 229–253.
Viles, H.A., 1995. Ecological perspectives on rock surface weathering: towards a conceptual model. Geomorphology 13, 21–35.
von Humboldt, A., 1812. Personal Narrative of Travels to the Equinoctial Regions of America During the Years 1799–1804 by Alexander von Humboldt and Aime Bonpland. Written in French by Alexander von Humboldt, vol. II (Translated and Edited by T. Ross in 1907). George Bell & Sons, London.
Walther, J., 1891. Die Denudation in der Wüste. Akademi der Wissenschaften: Mathematischk-Physicalische Klasse. Abhandlungen 16, 435–461.
Wang, X., Zeng, L., Wiens, M., Scholoßmacher, U., Jochum, K.P., Schröder, H.C., Müller, W.E.G., 2011. Evidence for a biogenic, microorganismal origin of rock varnish from the Gangdese Belt of Tibet. Micron 42, 401–411.
Wang, Z.L., Cowley, J.M., 1989. Simulating high-angle annular dark-field stem images including inelastic thermal diffuse scattering. Ultramicroscopy 31, 437–453.
Washburn, A.L., 1969. Case hardening. In: Washburn, A.L. (Ed.), Weathering, Frost Action and Patterned Ground in the Mesters District, Northeast Greenland. Reitzels, Copenhagen, p. 15.
White, C.H., 1924. Desert varnish. Am. J. Sci. 7, 413–420.
Wilhelmy, H., 1964. Cavernous rock surfaces in semi-arid and arid climates. Pak. Geogr. Rev. 19 (2), 8–13.
Woolnough, W.G., 1930. The influence of climate and topography in the formation and distribution of products of weathering. Geol. Mag. 67, 123–132.